

## **A HIGHER ORDER ANALYSIS OF A CLASS OF INHOMOGENEOUSLY FILLED CONDUCTING WAVEGUIDES**

**E. Khodapanah\* and S. Nikmehr**

Department of Electrical and Computer Engineering, University of Tabriz, Tabriz, Iran

**Abstract**—A higher order analysis is applied to solve the problem of a class of inhomogeneously-filled conducting waveguides. This includes an arbitrary but smooth hollow conducting waveguides and waveguides filled with layered inhomogeneous materials. The method employs a set of spline-harmonic basis functions and leads to one-dimensional integrals for system matrix elements. This fact along with the higher order nature of the basis functions provides an accurate method for the analysis of the aforementioned waveguides. The accuracy and the convergence behavior of the method are studied through several numerical examples and the results are compared with the exact solutions and with the results of Ansoft HFSS simulator to establish the validity of the proposed method.

### **1. INTRODUCTION**

Conducting waveguides of different cross sections have been used in microwave measurements [1–3] and in the design of various microwave components [3–7] specially, in the case of high power transmission of electromagnetic waves [3, 7]. A variety of analytical and numerical techniques have been applied to the analysis of uniform hollow conducting waveguides. Whereas application of analytical methods is limited to the analysis of waveguides with regular cross sections [8, 10], numerical methods have been extensively developed and successfully applied to the analysis of a conducting waveguide with a very general arbitrary shape cross section. Conducting waveguides filled with inhomogeneous materials have also found applications in the design

---

*Received 9 April 2011, Accepted 24 June 2011, Scheduled 3 July 2011*

\* Corresponding author: Ehsan Khodapanah (ekhodapanah@tabrizu.ac.ir).

of microwave components such as phase-shifters, attenuators, filters, etc. [11]. The problem of the propagation of electromagnetic waves in hollow conducting waveguides is reduced to the solution of the scalar Helmholtz equation subject to the Dirichlet and Neumann boundary conditions. This equation has been solved using the Rayleigh-Ritz method based on polynomial approximations [12, 13] and trigonometric basis functions [14]. Recently, this problem has been solved accurately by the method of external excitation in the simply or multiply connected regions and in the case of waveguides with boundary singularities [15]. Alternatively, this problem has been formulated as a surface integral equation and solved by the application of the method of moments [16]. The same approach has been applied for a class of conducting waveguides which are partially filled with pieces of homogeneous materials [17]. For more general inhomogeneities, one can apply the well-known finite element method (FEM) to solve the vector wave equation which is free of any spurious solution [18, 19]. An integral equation formulation which leads to a linear matrix eigenvalue problem has also been applied to solve the problem of homogeneous arbitrary shape waveguides [20, 21]. In the category of inhomogeneous waveguides, a bi-orthonormal basis method has also been applied to analyze inhomogeneously dielectric filled waveguides [22, 23].

It is known that the higher order methods provide faster convergence and more accurate results for a given number of unknowns in the numerical analysis of different electromagnetic problems [24–27]. In this work, we first define a class of inhomogeneous waveguides including arbitrarily but smoothly shaped single conductor waveguides filled with layered inhomogeneous materials and then apply a higher order numerical approach to analyze the propagation of electromagnetic waves inside these waveguides. The rest of the paper is organized as follows. In Section 2, the definition of the problem is presented. The analyses of homogeneous and inhomogeneous waveguides are described in Sections 3 and 4 respectively. Numerical results are given in Section 5. Finally, the conclusion is given in Section 6.

## 2. A CURVILINEAR COORDINATE SYSTEM

In order to define the cross sectional geometry of our uniform waveguides, we start by defining a curvilinear coordinate system. The fundamental curve for constructing an appropriate coordinate system conforming the waveguide boundaries is defined by  $\rho = \rho_1(\varphi)$  in the polar coordinates, where  $\rho_1(\varphi)$  is an arbitrary smooth and periodic function of  $\varphi$  which is assumed to have a non-zero value for any  $\varphi$  in

$[0, 2\pi]$ . Considering the closed curve,  $\rho = \rho_1(\varphi)$ , one can readily define a non-orthogonal curvilinear coordinate system  $u - \varphi$  as

$$\begin{cases} \rho = u\rho_1(\varphi) \\ \varphi = \varphi \end{cases} \quad 0 \leq u < \infty, \quad 0 \leq \varphi \leq 2\pi \quad (1)$$

Using the  $u - \varphi$  coordinate system defined in (1) we can define a class of inhomogeneous waveguides as follows. The inner and outer conductors of the waveguide which are assumed to be perfect electric conductors (PEC's) are located at  $u = u_1$  and  $u = u_2$  (constant  $u$  curves) respectively, and the region between two conductors is filled with an inhomogeneous material characterized by  $\epsilon_r(u)$  and  $\mu_r(u)$ . Also to this definition we add a case where the inner conductor is removed (single conductor waveguide).

It is also possible to define an orthogonal curvilinear coordinate system  $u - v$  as the following

$$\begin{cases} \rho = u\rho_1(\varphi) \\ \ln\left(\frac{u}{u_1}\right) = -\int_v^\varphi \left(\frac{\rho_1(\varphi')}{\rho_1'(\varphi')} + \frac{\rho_1'(\varphi')}{\rho_1(\varphi')}\right) d\varphi' \\ (|v - \varphi| \text{ is minimum}) \end{cases} \quad 0 \leq u < \infty, \quad 0 \leq v \leq 2\pi \quad (2)$$

where  $\rho_1'(\cdot)$  represents the derivative of  $\rho_1$  with respect to its argument and  $u_1$  can be selected arbitrarily (e.g., the inner or outer conductor of the waveguide in a given analysis). It is clear from (2) that the  $u - v$  system has the same  $u$  coordinate as the  $u - \varphi$  system in (1) and is obtained by finding a family of curves (constant  $v$  curves) which are orthogonal to the constant  $u$  curves defined in (1). The definition of the original problem in the  $u - v$  system is the same as that in the  $u - \varphi$  system. It is known from (2) that the  $\rho$  and  $\varphi$  and consequently the  $x$  and  $y$  are functions of  $u$  and  $v$  and hence the  $u - v$  system in (2) can be equivalently represented as

$$\begin{cases} x = x(u, v) \\ y = y(u, v) \end{cases} \quad (3)$$

where the functions  $x(u, v)$  and  $y(u, v)$  are known from (2) implicitly. Despite this later fact, the metric coefficients and unit vectors in the  $u - v$  system (which are necessary for vectorial analysis of the problem) can be obtained explicitly as

$$h_1 = \frac{\rho_1(\varphi)^2}{\sqrt{\rho_1(\varphi)^2 + \rho_1'(\varphi)^2}}, \quad h_2 = u\sqrt{\rho_1(\varphi)^2 + \rho_1'(\varphi)^2}\varphi_v \quad (4)$$

$$\hat{u} = \frac{1}{h_1}(x_u\hat{x} + y_u\hat{y}), \quad \hat{v} = \frac{1}{h_2}(x_v\hat{x} + y_v\hat{y}) \quad (5)$$

where the subscripts in the  $x$ ,  $y$ , and  $\varphi$  represent the partial derivatives and  $\varphi_v$  is as follows

$$\varphi_v = \left( \frac{\partial \varphi}{\partial v} \right)_u = \frac{\frac{\rho_1(v)}{\rho'_1(v)} + \frac{\rho'_1(v)}{\rho_1(v)}}{\frac{\rho_1(\varphi)}{\rho'_1(\varphi)} + \frac{\rho'_1(\varphi)}{\rho_1(\varphi)}} \quad (6)$$

### 3. HOMOGENEOUS WAVEGUIDES

When the waveguide is filled with a homogeneous material (i.e.,  $\epsilon_r$  and  $\mu_r$  have constant values), the problem is reduced to the solution of the two-dimensional scalar Helmholtz equation with the homogeneous Dirichlet and Neumann boundary conditions for TM and TE waves respectively. Mathematically, we should solve the following eigenvalue problem

$$\nabla^2 \psi + k_c^2 \psi = 0 \quad \begin{cases} \psi = 0 & \text{TM case} \\ \frac{\partial \psi}{\partial n} = 0 & \text{TE case} \end{cases} \quad \text{at } u = u_1 \text{ and } u_2 \quad (7)$$

where  $k_c$  is the unknown cutoff wavenumber which should be determined and  $\hat{n}$  is the outward unit normal of the waveguide boundaries. In order to solve the eigenvalue problem (7) numerically, we first expand the unknown function  $\psi$  as a sum of known basis functions with unknown coefficients. To this end, a set of spline-harmonic basis functions in the  $u-\varphi$  system is adopted as the following

$$\psi(u, \varphi) \cong \sum_{i=1}^{S_g+3} \sum_{n=-N}^N a_i^n S_i^4(u) e^{jn\varphi} \quad (8)$$

where  $S_i^4$  is the  $i$ th B-spline of order 4 (cubic B-spline) constructed on a uniform  $S_g$ -segment grid in the interval  $[u_1, u_2]$  [28]. To impose the Dirichlet boundary condition, we eliminate the two inhomogeneous cubic spline basis functions related to the two end points of the interval (i.e.,  $u_1$  and  $u_2$ ). Substituting (8) into (7) and applying Galerkin's method based on the Hilbert inner product, we obtain the following matrix eigenvalue equation for the unknown coefficients  $a_i^n$  and the unknown eigenvalues  $k_c$

$$Ax = k_c^2 Bx \quad (9)$$

where  $x = [a_1^{-N}, a_2^{-N}, \dots, a_{S_g+3}^N]^T$  is the vector of unknown coefficients and the elements of  $A$  and  $B$  are given by

$$\begin{aligned}
 A^{i_1 i_2 n_1 n_2} = & \int_{u_1}^{u_2} u (S_{i_1}^4(u))' (S_{i_2}^4(u))' du \int_0^{2\pi} \left(1 + \left(\frac{\rho_1'}{\rho_1}\right)^2\right) e^{j(n_2-n_1)\varphi} d\varphi \\
 & + \int_{u_1}^{u_2} S_{i_1}^4(u) (S_{i_2}^4(u))' du \int_0^{2\pi} j n_1 \frac{\rho_1'}{\rho_1} e^{j(n_2-n_1)\varphi} d\varphi \\
 & - \int_{u_1}^{u_2} (S_{i_1}^4(u))' S_{i_2}^4(u) du \int_0^{2\pi} j n_2 \frac{\rho_1'}{\rho_1} e^{j(n_2-n_1)\varphi} d\varphi \\
 & + \int_{u_1}^{u_2} \frac{S_{i_1}^4(u) S_{i_2}^4(u)}{u} du \int_0^{2\pi} n_1 n_2 e^{j(n_2-n_1)\varphi} d\varphi \quad (10)
 \end{aligned}$$

$$B^{i_1 i_2 n_1 n_2} = \int_{u_1}^{u_2} u S_{i_1}^4(u) S_{i_2}^4(u) du \int_0^{2\pi} \rho_1^2 e^{j(n_2-n_1)\varphi} d\varphi \quad (11)$$

(10) and (11) show that the two-dimensional integrals appearing in the elements of  $A$  and  $B$  are reduced to the products of one-dimensional integrals which is not a case when we try to solve the problem in the orthogonal  $u-v$  system. It is also found from (10) and (11) that  $A$  and  $B$  are Hermitian matrices which can be converted to real and symmetric matrices if we replace the complex harmonics  $e^{jn\varphi}$  in (8) by real harmonics  $\sin(n\varphi)$  and  $\cos(n\varphi)$ .

The matrices  $A$  and  $B$  are filled as follows. First we define two sets of matrices called  $U$  and  $\Phi$  matrices as

$$U_1^{i_1 i_2} = \int_{u_1}^{u_2} u (S_{i_1}^4(u))' (S_{i_2}^4(u))' du \quad (12)$$

$$U_2^{i_1 i_2} = \int_{u_1}^{u_2} S_{i_1}^4(u) (S_{i_2}^4(u))' du \quad (13)$$

$$U_3^{i_1 i_2} = \int_{u_1}^{u_2} \frac{S_{i_1}^4(u) S_{i_2}^4(u)}{u} du \quad (14)$$

$$U_4^{i_1 i_2} = \int_{u_1}^{u_2} u S_{i_1}^4(u) S_{i_2}^4(u) du \quad (15)$$

$$\Phi_1^{n_1 n_2} = \int_0^{2\pi} \left( 1 + \left( \frac{\rho'_1}{\rho_1} \right)^2 \right) e^{j(n_2 - n_1)\varphi} d\varphi \quad (16)$$

$$\Phi_2^{n_1 n_2} = \int_0^{2\pi} \frac{\rho'_1}{\rho_1} e^{j(n_2 - n_1)\varphi} d\varphi \quad (17)$$

$$\Phi_3^{n_1 n_2} = \int_0^{2\pi} e^{j(n_2 - n_1)\varphi} d\varphi \quad (18)$$

$$\Phi_4^{n_1 n_2} = \int_0^{2\pi} \rho_1^2 e^{j(n_2 - n_1)\varphi} d\varphi \quad (19)$$

It is clear from (12)–(15) that the  $U$  matrices are sparse and their sparsity increases by increasing the number of segments. All of the non-zero elements in  $U$  matrices can be calculated analytically due to the piecewise polynomial nature of the B-splines. The elements of the  $\Phi$  matrices are functions of  $n_2 - n_1$  and hence only one row or column of each  $\Phi_i$  matrix should be calculated. Analytical calculation may not be possible or may be difficult in general, however, a simple numerical integration method can be applied for an arbitrary  $\rho_1(\varphi)$ . Finally, we expand linear combinations of  $U$  matrices with appropriate weights which are the elements of  $\Phi$  matrices to fill out the matrices  $A$  and  $B$  in (9). The aforementioned procedure implies that the matrices  $A$  and  $B$  can be filled in a very fast manner.

The elements of  $\Phi_i$  in (16)–(19) show that for a circular waveguide all of the harmonics are decoupled. When the value of  $\min |\hat{v} \cdot \hat{\varphi}| = \min 1/\sqrt{1 + (\rho'_1/\rho_1)^2}$  which is a measure of the deviation of the waveguide geometry from a circular waveguide decreases from unity or equivalently  $\max |\rho'_1/\rho_1|$  increases from zero, the range of the harmonics which are strongly coupled to each other increases and consequently the number of harmonics required to solve the problem for a given accuracy increases.

Finally, we should mention that the analysis of a single conductor waveguide can be performed in the same manner as that described above except that we should select  $u_1 = 0$  and note that the value of  $\nabla\psi$  which represents the transverse field components must be

finite at the origin (i.e., at  $u = 0$ ). This latter fact means that in the approximation expression in (8) we should retain the left inhomogeneous cubic B-spline for the constant harmonic and eliminate it for other harmonics for both Dirichlet and Neumann problems.

#### 4. INHOMOGENEOUS WAVEGUIDES

For an inhomogeneous waveguide, we solve the vector wave equation for the electric field. Assuming that the electric field to be of the form  $\vec{E}(x, y, z, t) = (\vec{e}_t(x, y) + e_z(x, y)\hat{z})e^{j(\omega t - k_z z)}$  the vector wave equation is reduced to

$$\begin{aligned} \nabla \times \left( \frac{1}{\mu_r} \nabla \times \vec{e}_t \right) + \nabla \times \left( \frac{1}{\mu_r} (\nabla e_z + jk_z \vec{e}_t) \times \hat{z} \right) \\ - jk_z \frac{1}{\mu_r} (\nabla e_z + jk_z \vec{e}_t) - k_0^2 \epsilon_r (\vec{e}_t + e_z \hat{z}) = 0 \end{aligned} \quad (20)$$

where  $k_0 = \omega\sqrt{\mu_0\epsilon_0}$  is the wavenumber in the free space and  $k_z$  is the unknown propagation constant. To solve Equation (20), we first divide the two-dimensional cross section of the waveguide into a number of layers with continuous  $\epsilon_r(u)$  and  $\mu_r(u)$ . The  $l$ th layer is an area which is determined by  $u_1^l \leq u \leq u_2^l$  and  $0 \leq \varphi \leq 2\pi$ . Then, we apply a set of spline-harmonic basis functions to approximate the unknown electric field components inside each layer.

An important note which should be considered is that the transverse field components should be approximated in such a way that the function  $\hat{z} \cdot \nabla \times \vec{e}_t$  be represented as a sum of complete set, to avoid the spurious solutions [18]. Also  $e_z$  should be approximated such that  $(\nabla e_z + jk_z \vec{e}_t)$  appears as a sum of complete set of basis functions [18]. In the orthogonal  $u - v$  system these requirements can be easily achieved by using the metric coefficients. In fact, we can select

$$\begin{aligned} \vec{e}_t &= \frac{1}{h_1} \sum_{i,n} a_i^n S_i^3(u) e^{jnv} \hat{u} + \frac{1}{h_2} \sum_{i,n} b_i^n S_i^4(u) e^{jnv} \hat{v} \\ e_z &= \sum_{i,n} c_i^n S_i^4(u) e^{jnv} \end{aligned} \quad (21)$$

and then apply Galerkin's method to convert Equation (20) to a generalized matrix eigenvalue problem. However, this procedure leads to expensive two-dimensional integrals for system matrix elements, which reduces the efficiency of the method.

An approximation on a set of curl-conforming spline-harmonic basis functions in the non-orthogonal  $u - \varphi$  system is given by

$$\begin{aligned}\vec{e}_t &= \frac{1}{h_1} \sum_{i,n} a_i^n S_i^3(u) e^{jn\varphi} \hat{u} + \frac{1}{\rho} \sum_{i,n} b_i^n S_i^4(u) e^{jn\varphi} \hat{\varphi} \\ e_z &= \sum_{i,n} c_i^n S_i^4(u) e^{jn\varphi}\end{aligned}\quad (22)$$

Now Galerkin's method based on the above approximations leads to one-dimensional integrals for system matrix elements, which can be calculated in a very fast manner. It is clear from (22) that the transverse component is approximated by two sets of non-orthogonal vector basis functions. In order to increase the accuracy of the method for a given number of unknowns in the case where the non-orthogonality of the geometry increases (i.e., when the value of  $\max |\hat{u} \cdot \hat{\varphi}| = \max 1/\sqrt{1 + (\rho_1/\rho'_1)^2}$  increases or  $\min |\rho_1/\rho'_1|$  decreases) we replace the  $\hat{\varphi}$  directed basis functions in (22) by the following ones

$$\frac{\varphi_v}{h_2} \left( 1 + \left( \frac{\rho'_1}{\rho_1} \right)^2 \right) S_i^4(u) e^{jn\varphi} \hat{v} \quad (23)$$

However, the testing functions should remain unchanged to avoid spurious solutions. Following the non-galerkin procedure described above, we can convert Equation (20) to the following matrix eigenvalue equation

$$\begin{bmatrix} A_{uu} & A_{uv} \\ A_{\varphi u} & A_{\varphi v} \end{bmatrix} \begin{bmatrix} a \\ b \end{bmatrix} = k_z^2 \begin{bmatrix} A_{uz}(A_{zz}^{-1}A_{zu}) - B_{uu} & A_{uz}(A_{zz}^{-1}A_{zv}) \\ A_{\varphi z}(A_{zz}^{-1}A_{zu}) - B_{\varphi u} & A_{\varphi z}(A_{zz}^{-1}A_{zv}) - B_{\varphi v} \end{bmatrix} \begin{bmatrix} a \\ b \end{bmatrix} \quad (24)$$

where  $a = [a_1^{-N}, a_2^{-N}, \dots, a_{l(S_g+2)}^N]^T$  and  $b = [b_1^{-N}, b_2^{-N}, \dots, b_{l(S_g+3)}^N]^T$  are the unknown vectors related to the transverse components ( $l$  is the number of layers) and the elements of the different matrices in (24) are given by

$$\begin{aligned}A_{uu}^{i_1 i_2 n_1 n_2} &= \int_{u_1}^{u_2} \frac{1}{\mu_r} \frac{S_{i_1}^3(u) S_{i_2}^3(u)}{u} du \int_0^{2\pi} \frac{n_1 n_2}{\rho_1^2} e^{j(n_2 - n_1)\varphi} d\varphi \\ &- k_0^2 \int_{u_1}^{u_2} \epsilon_r u S_{i_1}^3(u) S_{i_2}^3(u) du \int_0^{2\pi} \left( 1 + \left( \frac{\rho'_1}{\rho_1} \right)^2 \right) e^{j(n_2 - n_1)\varphi} d\varphi\end{aligned}\quad (25)$$

$$\begin{aligned}
A_{uv}^{i_1 i_2 n_1 n_2} &= \int_{u_1}^{u_2} \frac{1}{\mu_r} \frac{S_{i_1}^3(u) (S_{i_2}^4(u))'}{u} du \int_0^{2\pi} \frac{j n_1}{\rho_1^2} \left( 1 + \left( \frac{\rho_1'}{\rho_1} \right)^2 \right) e^{j(n_2 - n_1)\varphi} d\varphi \\
&\quad - \int_{u_1}^{u_2} \frac{1}{\mu_r} \frac{S_{i_1}^3(u) S_{i_2}^4(u)}{u^2} du \int_0^{2\pi} \frac{j n_1}{\rho_1^2} \left( \frac{\rho_1''}{\rho_1} - \left( \frac{\rho_1'}{\rho_1} \right)^2 + j n_2 \frac{\rho_1'}{\rho_1} \right) e^{j(n_2 - n_1)\varphi} d\varphi \quad (26)
\end{aligned}$$

$$\begin{aligned}
A_{uz}^{i_1 i_2 n_1 n_2} &= \int_{u_1}^{u_2} \frac{1}{\mu_r} u S_{i_1}^3(u) (S_{i_2}^4(u))' du \int_0^{2\pi} \left( 1 + \left( \frac{\rho_1'}{\rho_1} \right)^2 \right) e^{j(n_2 - n_1)\varphi} d\varphi \\
&\quad - \int_{u_1}^{u_2} \frac{1}{\mu_r} S_{i_1}^3(u) S_{i_2}^4(u) du \int_0^{2\pi} j n_2 \frac{\rho_1'}{\rho_1} e^{j(n_2 - n_1)\varphi} d\varphi \quad (27)
\end{aligned}$$

$$B_{uu}^{i_1 i_2 n_1 n_2} = \int_{u_1}^{u_2} \frac{1}{\mu_r} u S_{i_1}^3(u) S_{i_2}^3(u) du \int_0^{2\pi} \left( 1 + \left( \frac{\rho_1'}{\rho_1} \right)^2 \right) e^{j(n_2 - n_1)\varphi} d\varphi \quad (28)$$

$$\begin{aligned}
A_{\varphi u}^{i_1 i_2 n_1 n_2} &= - \int_{u_1}^{u_2} \frac{1}{\mu_r} \frac{(S_{i_1}^4(u))' S_{i_2}^3(u)}{u} du \int_0^{2\pi} \frac{j n_2}{\rho_1^2} e^{j(n_2 - n_1)\varphi} d\varphi \\
&\quad + k_0^2 \int_{u_1}^{u_2} \epsilon_r S_{i_1}^4(u) S_{i_2}^3(u) du \int_0^{2\pi} \frac{\rho_1'}{\rho_1} e^{j(n_2 - n_1)\varphi} d\varphi \quad (29)
\end{aligned}$$

$$\begin{aligned}
A_{\varphi v}^{i_1 i_2 n_1 n_2} &= \int_{u_1}^{u_2} \frac{1}{\mu_r} \frac{(S_{i_1}^4(u))' (S_{i_2}^4(u))'}{u} du \int_0^{2\pi} \frac{1}{\rho_1^2} \left( 1 + \left( \frac{\rho_1'}{\rho_1} \right)^2 \right) e^{j(n_2 - n_1)\varphi} d\varphi \\
&\quad - \int_{u_1}^{u_2} \frac{1}{\mu_r} \frac{(S_{i_1}^4(u))' S_{i_2}^4(u)}{u^2} du \int_0^{2\pi} \frac{1}{\rho_1^2} \left( \frac{\rho_1''}{\rho_1} - \left( \frac{\rho_1'}{\rho_1} \right)^2 + j n_2 \frac{\rho_1'}{\rho_1} \right) e^{j(n_2 - n_1)\varphi} d\varphi \\
&\quad - k_0^2 \int_{u_1}^{u_2} \epsilon_r \frac{S_{i_1}^4(u) S_{i_2}^4(u)}{u} du \int_0^{2\pi} e^{j(n_2 - n_1)\varphi} d\varphi \quad (30)
\end{aligned}$$

$$\begin{aligned}
A_{\varphi z}^{i_1 i_2 n_1 n_2} &= - \int_{u_1}^{u_2} \frac{1}{\mu_r} S_{i_1}^4(u) (S_{i_2}^4(u))' du \int_0^{2\pi} \frac{\rho_1'}{\rho_1} e^{j(n_2 - n_1)\varphi} d\varphi \\
&\quad + \int_{u_1}^{u_2} \frac{1}{\mu_r} \frac{S_{i_1}^4(u) S_{i_2}^4(u)}{u} du \int_0^{2\pi} j n_2 e^{j(n_2 - n_1)\varphi} d\varphi \quad (31)
\end{aligned}$$

$$B_{\varphi u}^{i_1 i_2 n_1 n_2} = - \int_{u_1}^{u_2} \frac{1}{\mu_r} S_{i_1}^4(u) S_{i_2}^3(u) du \int_0^{2\pi} \frac{\rho_1'}{\rho_1} e^{j(n_2-n_1)\varphi} d\varphi \quad (32)$$

$$B_{\varphi v}^{i_1 i_2 n_1 n_2} = \int_{u_1}^{u_2} \frac{1}{\mu_r} \frac{S_{i_1}^4(u) S_{i_2}^4(u)}{u} du \int_0^{2\pi} e^{j(n_2-n_1)\varphi} d\varphi \quad (33)$$

$$\begin{aligned} A_{zz}^{i_1 i_2 n_1 n_2} = & \int_{u_1}^{u_2} \frac{1}{\mu_r} u (S_{i_1}^4(u))' (S_{i_2}^4(u))' du \int_0^{2\pi} \left(1 + \left(\frac{\rho_1'}{\rho_1}\right)^2\right) e^{j(n_2-n_1)\varphi} d\varphi \\ & + \int_{u_1}^{u_2} \frac{1}{\mu_r} S_{i_1}^4(u) (S_{i_2}^4(u))' du \int_0^{2\pi} j n_1 \frac{\rho_1'}{\rho_1} e^{j(n_2-n_1)\varphi} d\varphi \\ & - \int_{u_1}^{u_2} \frac{1}{\mu_r} (S_{i_1}^4(u))' S_{i_2}^4(u) du \int_0^{2\pi} j n_2 \frac{\rho_1'}{\rho_1} e^{j(n_2-n_1)\varphi} d\varphi \\ & + \int_{u_1}^{u_2} \frac{1}{\mu_r} \frac{S_{i_1}^4(u) S_{i_2}^4(u)}{u} du \int_0^{2\pi} n_1 n_2 e^{j(n_2-n_1)\varphi} d\varphi \\ & - k_0^2 \int_{u_1}^{u_2} \epsilon_r u S_{i_1}^4(u) S_{i_2}^4(u) du \int_0^{2\pi} \rho_1^2 e^{j(n_2-n_1)\varphi} d\varphi \end{aligned} \quad (34)$$

$$\begin{aligned} A_{zu}^{i_1 i_2 n_1 n_2} = & \int_{u_1}^{u_2} \frac{1}{\mu_r} u (S_{i_1}^4(u))' S_{i_2}^3(u) du \int_0^{2\pi} \left(1 + \left(\frac{\rho_1'}{\rho_1}\right)^2\right) e^{j(n_2-n_1)\varphi} d\varphi \\ & + \int_{u_1}^{u_2} \frac{1}{\mu_r} S_{i_1}^4(u) S_{i_2}^3(u) du \int_0^{2\pi} j n_1 \frac{\rho_1'}{\rho_1} e^{j(n_2-n_1)\varphi} d\varphi \end{aligned} \quad (35)$$

$$A_{zv}^{i_1 i_2 n_1 n_2} = - \int_{u_1}^{u_2} \frac{1}{\mu_r} \frac{S_{i_1}^4(u) S_{i_2}^4(u)}{u} du \int_0^{2\pi} j n_1 e^{j(n_2-n_1)\varphi} d\varphi \quad (36)$$

To fill the matrices in (24) we do as follows. First, two sets of matrices i.e., U matrices and  $\Phi$  matrices are defined. The  $\Phi$  matrices are independent of layers and have the same properties as those of previous section. The U matrices are calculated for a complete set of B-splines in each layer. This can be performed analytically, when  $\epsilon_r$  and  $\mu_r$  have simple forms (e.g., in a partially filled waveguide)

or numerically, when analytical calculations are not possible. Then, we put  $U$  matrices of the same types of different layers on the main diagonals of larger  $U$  matrices to construct the  $U$  matrices of the whole structure. Imposition of the boundary and continuity conditions are performed by combining the two rows or columns of the global  $U$  matrices related to the two inhomogeneous cubic B-splines of two adjacent layers and by eliminating the rows and columns related to cubic B-splines which are adjacent to the waveguide walls. Finally, we expand the linear combinations of the global  $U$  matrices by proper weights which are the values of the  $\Phi$  matrices to obtain the matrices in (24). The generalized eigenvalue problem in (24) is solved by using the `sparm` function in the MATLAB partial differential equation (PDE) toolbox based on the implicitly restarted Arnoldi method.

At the end of this section, we mention that a single conductor inhomogeneous waveguide is analyzed by the same method described above for a two-conductor waveguide except that all of the electric and magnetic field components must remain finite at the origin. This is achieved by eliminating the left inhomogeneous cubic spline basis and testing functions in the approximation of the components  $e_v$  and  $e_\varphi$  in the first layer and by imposing the same conditions on  $e_z$  as those imposed on the scalar function  $\psi$  in the previous section. Also, we should impose the condition  $\lim_{u \rightarrow 0} u (\hat{z} \cdot \nabla \times \vec{e}_t) = 0$ . This latter condition means that a new set of equations should be produced and added to the system of equations in (24). In this work, we impose this condition approximately. In fact, we select the lower limit of the first layer  $u_1^l$  not at the origin but at the point  $u_1^l = \varepsilon$ , where  $\varepsilon$  is a very small number (e.g.,  $\varepsilon = 10^{-100}$ ) and apply the same algorithm described for a two-conductor waveguide. In this way, the condition  $u (\hat{z} \cdot \nabla \times \vec{e}_t) = 0$  is imposed at  $u = \varepsilon$  as a natural boundary condition which is a good approximation to the finite field condition at the origin.

## 5. NUMERICAL RESULTS

First, let us consider the case in which the main period of the function  $\rho_1(\varphi)$  is smaller than  $2\pi$  i.e., is  $2\pi/q$  where  $q$  is an integer larger than unity. In this special case, the main problem is reduced to  $q$  decoupled problems, each is constructed by a set of coupled harmonics with the indices  $m, m \pm q, m \pm 2q, \dots$  in which it is assumed that the minimum non-negative index is  $m$ . Every set of coupled harmonics which is characterized by  $m$  leads to a set of modes in the waveguide which is called the  $m$ th mode family. It is clear that the  $m$ th and the  $(q - m)$ th mode families are degenerate. Therefore, it is sufficient to consider only the zeroth, first,  $\dots$ ,  $[q/2]$ th mode families in this

special case to take advantages of the symmetry of the waveguide in the  $\varphi$  direction.

As the first example, we investigate the accuracy of the method on the number of spline segments,  $S_g$ , by considering the problem of a unit circular waveguide and a circular coaxial waveguide with  $u_1 = 0.5$  and  $u_2 = 1$ . The cutoff wavenumbers of lower order modes for the both cases are compared with the exact results for different numbers of segments and the relative errors are listed in Tables 1 and 2. Tables 1 and 2 show that for a same number of segments and a same mode type the method is more accurate for the coaxial waveguide in comparison to the circular waveguide when the values of the cutoff wavenumbers of the both structures are near to each other. However, the convergence rate is almost the same for the both cases.

**Table 1.** Relative errors of the cutoff wavenumbers of the lower order modes for a unit circular waveguide.

Mode	$k_c^{exact} \text{ (m}^{-1}\text{)}$	Relative error of proposed method			
		$S_g = 4$	$S_g = 8$	$S_g = 16$	$S_g = 32$
$TM_{01}$	2.404825557695773	$9.1 \times 10^{-8}$	$1.3 \times 10^{-9}$	$2 \times 10^{-11}$	$5.5 \times 10^{-13}$
$TM_{02}$	5.520078110286311	$8.9 \times 10^{-5}$	$9.5 \times 10^{-7}$	$1.3 \times 10^{-8}$	$1.9 \times 10^{-10}$
$TM_{03}$	8.653727912911013	$2 \times 10^{-3}$	$2.5 \times 10^{-5}$	$2.9 \times 10^{-7}$	$4.1 \times 10^{-9}$
$TM_{11}$	3.831705970207512	$5.1 \times 10^{-6}$	$6.1 \times 10^{-8}$	$8.8 \times 10^{-10}$	$1.3 \times 10^{-11}$
$TM_{12}$	7.015586669815620	$5.5 \times 10^{-4}$	$5.1 \times 10^{-6}$	$6.3 \times 10^{-8}$	$9.2 \times 10^{-10}$
$TM_{21}$	5.135622301840683	$3.2 \times 10^{-5}$	$3.4 \times 10^{-7}$	$4.6 \times 10^{-9}$	$6.9 \times 10^{-11}$
$TM_{22}$	8.417244140399864	$1.4 \times 10^{-3}$	$1.4 \times 10^{-5}$	$1.6 \times 10^{-7}$	$2.3 \times 10^{-9}$
$TM_{31}$	6.380161895923983	$1.1 \times 10^{-4}$	$1 \times 10^{-6}$	$1.3 \times 10^{-8}$	$1.9 \times 10^{-10}$
$TM_{41}$	7.588342434503804	$2.1 \times 10^{-4}$	$2.1 \times 10^{-6}$	$2.5 \times 10^{-8}$	$3.6 \times 10^{-10}$
$TM_{51}$	8.771483815959954	$2.2 \times 10^{-4}$	$3.7 \times 10^{-6}$	$4.4 \times 10^{-8}$	$6.2 \times 10^{-10}$
$TE_{01}$	3.831705970207512	$5.2 \times 10^{-6}$	$8.3 \times 10^{-8}$	$1.3 \times 10^{-9}$	$2.2 \times 10^{-11}$
$TE_{02}$	7.015586669815620	$4.8 \times 10^{-4}$	$5.2 \times 10^{-6}$	$7.2 \times 10^{-8}$	$1.1 \times 10^{-9}$
$TE_{11}$	1.841183781340659	$4.4 \times 10^{-8}$	$7.7 \times 10^{-10}$	$1.3 \times 10^{-11}$	$3 \times 10^{-13}$
$TE_{12}$	5.331442773525033	$5.7 \times 10^{-5}$	$7.1 \times 10^{-7}$	$1.1 \times 10^{-8}$	$1.7 \times 10^{-10}$
$TE_{21}$	3.054236928227140	$6 \times 10^{-7}$	$9.1 \times 10^{-9}$	$1.5 \times 10^{-10}$	$2.9 \times 10^{-12}$
$TE_{22}$	6.706133194158459	$2.4 \times 10^{-4}$	$2.3 \times 10^{-6}$	$3.3 \times 10^{-8}$	$5.1 \times 10^{-10}$
$TE_{31}$	4.201188941210528	$4.1 \times 10^{-6}$	$4.4 \times 10^{-8}$	$6.5 \times 10^{-10}$	$1.1 \times 10^{-11}$
$TE_{41}$	5.317553126083994	$1.3 \times 10^{-5}$	$1 \times 10^{-7}$	$1.4 \times 10^{-9}$	$2.3 \times 10^{-11}$
$TE_{51}$	6.415616375700241	$3.2 \times 10^{-5}$	$2.1 \times 10^{-7}$	$2.7 \times 10^{-9}$	$4.2 \times 10^{-11}$
$TE_{61}$	7.501266144684148	$6.5 \times 10^{-5}$	$3.9 \times 10^{-7}$	$4.6 \times 10^{-9}$	$7 \times 10^{-11}$

**Table 2.** Relative errors of the cutoff wavenumbers of the lower order modes for a circular coaxial waveguide with  $u_1 = 0.5$  and  $u_2 = 1$ .

Mode	$k_c^{exact} \text{ (m}^{-1}\text{)}$	Relative error of proposed method		
		$S_g = 4$	$S_g = 8$	$S_g = 16$
$TM_{01}$	6.246061839191384	$3.5 \times 10^{-6}$	$4.9 \times 10^{-8}$	$7.5 \times 10^{-10}$
$TM_{02}$	12.54687142798436	$4.5 \times 10^{-4}$	$4.7 \times 10^{-6}$	$6.2 \times 10^{-8}$
$TM_{11}$	6.393156761621269	$3.4 \times 10^{-6}$	$4.6 \times 10^{-8}$	$7 \times 10^{-10}$
$TM_{21}$	6.813842853135051	$3.4 \times 10^{-6}$	$4.2 \times 10^{-8}$	$6.1 \times 10^{-10}$
$TM_{31}$	7.457740136051091	$4 \times 10^{-6}$	$4.6 \times 10^{-8}$	$6.6 \times 10^{-10}$
$TM_{41}$	8.266730435360103	$5.2 \times 10^{-6}$	$6.2 \times 10^{-8}$	$9.1 \times 10^{-10}$
$TM_{51}$	9.190044424963240	$7.1 \times 10^{-6}$	$8.8 \times 10^{-8}$	$1.3 \times 10^{-9}$
$TM_{61}$	10.18892992360880	$9.6 \times 10^{-6}$	$1.2 \times 10^{-7}$	$1.9 \times 10^{-9}$
$TM_{71}$	11.23570779347832	$1.2 \times 10^{-5}$	$1.6 \times 10^{-7}$	$2.5 \times 10^{-9}$
$TM_{81}$	12.31130859721133	$1.6 \times 10^{-5}$	$2.1 \times 10^{-7}$	$3.2 \times 10^{-9}$
$TE_{01}$	6.393156761621269	$2.8 \times 10^{-6}$	$4.5 \times 10^{-8}$	$7.4 \times 10^{-10}$
$TE_{11}$	1.354672010273168	$4 \times 10^{-8}$	$7.6 \times 10^{-10}$	$1.4 \times 10^{-11}$
$TE_{12}$	6.564942382322760	$2.9 \times 10^{-6}$	$4.6 \times 10^{-8}$	$7.5 \times 10^{-10}$
$TE_{21}$	2.681204286668842	$1.3 \times 10^{-7}$	$2.5 \times 10^{-9}$	$4.6 \times 10^{-11}$
$TE_{22}$	7.062581616047449	$3.3 \times 10^{-6}$	$5.2 \times 10^{-8}$	$8.5 \times 10^{-10}$
$TE_{31}$	3.957754187823974	$2 \times 10^{-7}$	$3.9 \times 10^{-9}$	$7.5 \times 10^{-11}$
$TE_{32}$	7.840109097858155	$4.4 \times 10^{-6}$	$6.7 \times 10^{-8}$	$1.1 \times 10^{-9}$
$TE_{41}$	5.175227739588027	$2.6 \times 10^{-7}$	$4.9 \times 10^{-9}$	$9.2 \times 10^{-11}$
$TE_{51}$	6.338887081897594	$3.6 \times 10^{-7}$	$5.9 \times 10^{-9}$	$1.1 \times 10^{-10}$
$TE_{61}$	7.462157848409306	$5.5 \times 10^{-7}$	$7.8 \times 10^{-9}$	$1.3 \times 10^{-10}$

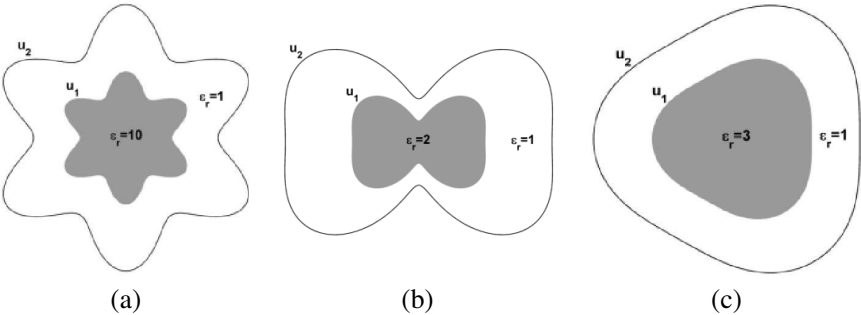


**Figure 1.** Geometries of the waveguides under study. (a)  $\rho_1 = 1 - 0.2 \cos(6\varphi)$ ,  $u_1/u_2 = 0.5$ . (b)  $\rho_1 = 1 + 0.4 \cos(2\varphi) - 0.2 \cos(4\varphi)$ ,  $u_1/u_2 = 0.5$ . (c)  $\rho_1 = 1 - 0.1 \cos(3\varphi)$ ,  $u_1/u_2$  is a parameter.

**Table 3.** Normalized propagation constant of the dominant mode for a partially filled coaxial waveguide with  $\rho_1(\varphi) = 1 - w \cos(4\varphi)$ ,  $u_1^1 = 1$ ,  $u_1^2 = 1.5$ ,  $u_2^1 = 1.5$ ,  $u_2^2 = 2$ ,  $\epsilon_r^1 = 2$ , and  $\epsilon_r^2 = 1$ , at the frequency  $k_0 = 2 \text{ (m}^{-1}\text{)}$ , for three different values of  $w$ . Error is calculated with respect to the most accurate result at the bottom of each group.

	Number of harmonics	$k_z/k_0$ for the dominant mode	Relative error
$w = 0.1$	3	1.225493210098283	$9.9 \times 10^{-5}$
	5	1.225612770232861	$1.5 \times 10^{-6}$
	7	1.225614590304224	$1.8 \times 10^{-8}$
	9	1.225614569582404	$1 \times 10^{-9}$
	11	1.225614568363040	$3.9 \times 10^{-11}$
	13	1.225614568316376	$1.7 \times 10^{-12}$
	15	1.225614568314887	$5.2 \times 10^{-14}$
	17	1.225614568314823	-
$w = 0.3$	3	1.218804214386114	$3.3 \times 10^{-3}$
	7	1.222851721084015	$2.6 \times 10^{-5}$
	11	1.222885364877253	$1 \times 10^{-6}$
	15	1.222884340917631	$1.9 \times 10^{-7}$
	19	1.222884124236825	$1.2 \times 10^{-8}$
	23	1.222884112093381	$1.7 \times 10^{-9}$
	27	1.222884110263445	$1.9 \times 10^{-10}$
	31	1.222884110057294	$2 \times 10^{-11}$
	35	1.222884110035376	$1.8 \times 10^{-12}$
	39	1.222884110033236	-
$w = 0.6$	11	1.218105629434032	$7.1 \times 10^{-4}$
	21	1.218980921113077	$7.9 \times 10^{-6}$
	31	1.218973149429752	$1.6 \times 10^{-6}$
	41	1.218971729050500	$4.1 \times 10^{-7}$
	51	1.218971297905761	$6 \times 10^{-8}$
	61	1.218971229121749	$3.4 \times 10^{-9}$
	71	1.218971224721125	$2.5 \times 10^{-10}$
	81	1.218971224951328	$2.6 \times 10^{-11}$
	91	1.218971225022000	$1.5 \times 10^{-12}$
	101	1.218971225020170	-

To study the accuracy and the convergence behavior of the method on the number of harmonics, we consider the problem of a partially filled coaxial waveguide with  $\rho_1(\varphi) = 1 - w \cos(4\varphi)$ ,  $u_1^1 = 1$ ,  $u_1^2 = 1.5$ ,  $u_2^1 = 1.5$ ,  $u_2^2 = 2$ ,  $\epsilon_r^1 = 2$ , and  $\epsilon_r^2 = 1$ , where the superscripts 1 and 2 represent respectively the first and the second layers in the waveguide. The value of  $w$  is a measure of the deviation from a circular waveguide. In fact, for a circular waveguide we have  $w = 0$ . As  $w$  increases from zero the deviation from a circular case also increases. Therefore, we

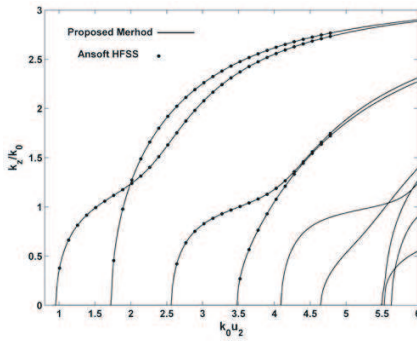


**Figure 2.** Normalized propagation constants of the lower order modes of the zeroth mode family of the waveguide in Fig. 1(a).

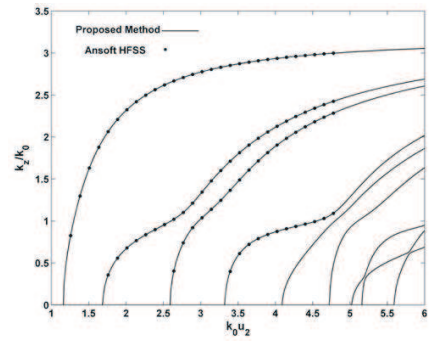


**Figure 3.** Normalized propagation constants of the lower order modes of the first mode family of the waveguide in Fig. 1(a).

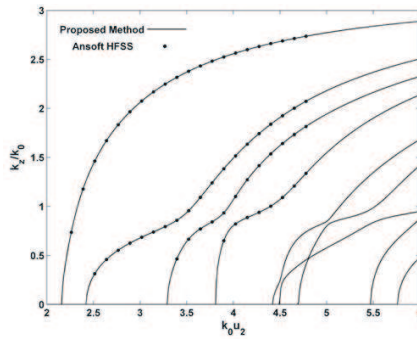


**Figure 4.** Normalized propagation constants of the lower order modes of the second mode family of the waveguide in Fig. 1(a).

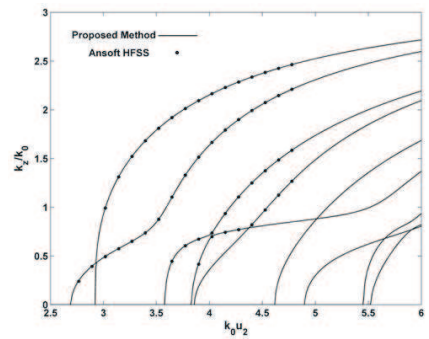


**Figure 5.** Normalized propagation constants of the lower order modes of the third mode family of the waveguide in Fig. 1(a).

consider three different cases i.e.,  $w = 0.1$ ,  $w = 0.3$ , and  $w = 0.6$  which are respectively related to a small, an intermediate, and a large deviation from a circular waveguide. The results for all three cases are shown in Table 3 where the normalized propagation constant ( $k_z/k_0$ ) of the dominant mode is given at  $k_0 = 2 \text{ (m}^{-1}\text{)}$  (the dominant mode belongs to the zeroth mode family). Table 3 shows that for a given accuracy the number of required harmonics increases when the value of  $w$  increases. Also the convergence rate and the computational efficiency of the method decrease by  $w$ .

Finally, we consider three single conductor waveguides partially filled with dielectric materials. The geometries of these waveguides are shown in Fig. 1. The normalized propagation constants of different

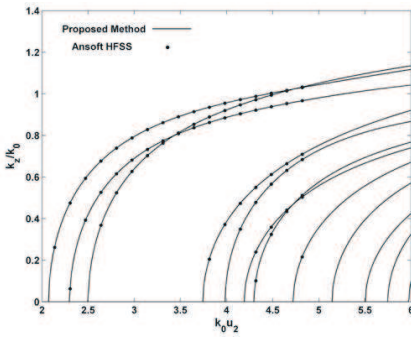


**Figure 6.** Normalized propagation constants of the lower order modes of the zeroth mode family of the waveguide in Fig. 1(b).

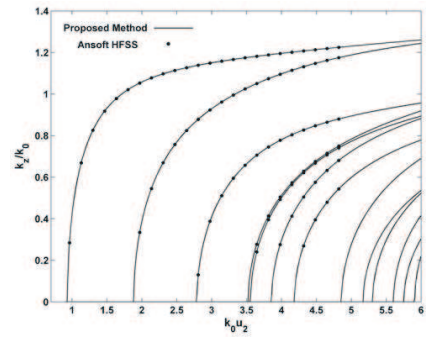


**Figure 7.** Normalized propagation constants of the lower order modes of the first mode family of the waveguide in Fig. 1(b).

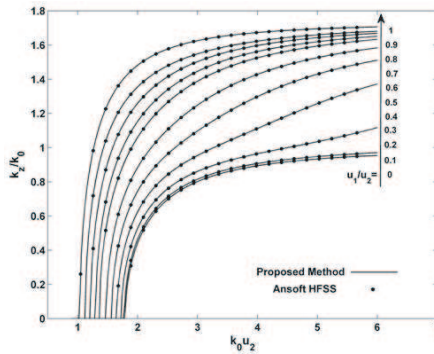


**Figure 8.** Normalized propagation constants of the dominant mode of the waveguide in Fig. 1(c) for different values of  $u_1/u_2$ .

mode families of Fig. 1(a) are shown in Figs. 2–5 and for Fig. 1(b) are shown in Figs. 6 and 7 and for the dominant mode of Fig. 1(c) for different filling values ( $u_1/u_2$ ) are shown in Fig. 8. All of the results are compared with the Ansoft HFSS results and excellent agreement is observed for all the cases. The accuracy of the results obtained by HFSS is 3 or 4 significant digits for the problems in Fig. 1. For the same accuracy, our method is at least a hundred times faster showing the efficiency of the proposed method.

## 6. CONCLUSION

Spline-harmonic functions were applied for an accurate analysis of a class of inhomogeneously-filled conducting waveguides. By increasing or decreasing the order of B-splines, one can easily increase or decrease the order of the method. The efficiency of the proposed method of analysis strongly depends on the amount of deviation from a circular waveguide. The method is very efficient up to an intermediate deviation from circular case, and still remains relatively efficient for a large deviation. The proposed method can also be applied to the analysis of a sectorial waveguide of the same class. However, we should apply Galerkin's method to make the imposition of the PEC boundary condition easier.

## REFERENCES

1. Hasar, U. C., "Thickness-independent automated constitutive parameters extraction of thin solid and liquid materials from waveguide measurements," *Progress In Electromagnetics Research*, Vol. 92, 17–32, 2009.
2. Hasar, U. C., "Thickness-independent complex permittivity determination of partially filled thin dielectric materials into rectangular waveguides," *Progress In Electromagnetics Research*, Vol. 93, 189–203, 2009.
3. Kancleris, Z., G. Slekas, V. Tamosiunas, and M. Tamosiuniene, "Resistive sensor for high power microwave pulse measurement of TE<sub>01</sub> mode in circular waveguide," *Progress In Electromagnetics Research*, Vol. 92, 267–280, 2009.
4. Sangster, A. J. and J. Grant, "Mode degeneracy in circular cylindrical ridge waveguides," *Progress In Electromagnetics Research Letters*, Vol. 9, 75–83, 2009.
5. Khalilpour, J. and M. Hakkak, "Controllable waveguide bandstop filter using s-shaped ring resonators," *Journal of Electromagnetic Waves and Applications*, Vol. 24, Nos. 5–6, 587–596, 2010.

6. Siakavara, K. and C. Damianidis, "Microwave filtering in waveguides loaded with artificial single or double negative materials realized with dielectric spherical particles in resonance," *Progress In Electromagnetics Research*, Vol. 95, 103–120, 2009.
7. Pozar, D. M., *Microwave Engineering*, John Wiley & Sons, Hoboken, NJ, 2005.
8. Harrington, R. F., *Time Harmonic Electromagnetic Fields*, McGraw-Hill, New York, 1961.
9. Skobelev, S. P. and P. S. Kildal, "A new type of the quasi-TEM eigenmodes in a rectangular waveguide with one corrugated hard wall," *Progress In Electromagnetics Research*, Vol. 102, 143–157, 2010.
10. Xu, J., W. X. Wang, L. N. Yue, Y. B. Gong, and Y. Y. Wei, "Electromagnetic wave propagation in an elliptical chiroferrite waveguide," *Journal of Electromagnetic Waves and Applications*, Vol. 23, Nos. 14–15, 2021–2030, 2009.
11. Ma, J. G., "Numerical analysis of the characteristics of TE-modes of waveguides loaded with inhomogeneous dielectrics," *IEE Proc. PtH*, Vol. 138, 109–112, 1991.
12. Bulley, R. M., "Analysis of the arbitrary shaped waveguide by polynomial approximation," *IEEE Trans. Microwave Theory Tech.*, Vol. 18, No. 12, 1022–1028, Dec. 1970.
13. Lin, S. L., L. W. Li, T. S. Yeo, and M. S. Leong, "Analysis of hollow conducting waveguides using superquadric functions — A unified representation," *IEEE Trans. Microwave Theory Tech.*, Vol. 48, No. 5, 876–880, May 2000.
14. Thomas, D. T., "Functional approximations for solving boundary value problems by computer," *IEEE Trans. Microwave Theory Tech.*, Vol. 17, No. 8, 447–454, Aug. 1969.
15. Reutskiy, S. Y., "The methods of external excitation for analysis of arbitrarily-shaped hollow conducting waveguides," *Progress In Electromagnetics Research*, Vol. 82, 203–226, 2008.
16. Kim, C. Y., S. D. Yu, R. F., Harrington, J. W. Ra, and S. Y. Lee, "Computation of waveguide modes for waveguides of arbitrary cross-section," *IEE Proc. PtH*, Vol. 137, No. 2, 145–149, Apr. 1990.
17. Paul, S. S., M., Goggans, and A. A., Kishk, "Computation of cutoff wavenumbers for partially filled waveguides of arbitrary cross section using surface integral formulations and the method of moments," *IEEE Trans. Microwave Theory Tech.*, Vol. 41, No. 6–7, 1111–1118, Jun./Jul. 1993.
18. Lee, J. F., D. K., Sun, and Z. J., Cendes, "Full-wave analysis

- of dielectric waveguides using tangential vector finite elements," *IEEE Trans. Microwave Theory Tech.*, Vol. 39, No. 8, 1262–1271, Aug. 1991.
19. Lee, J. F., "Finite element analysis of lossy dielectric waveguides" *IEEE Trans. Microwave Theory Tech.*, Vol. 42, No. 6, 1025–1031, Jun. 1994.
  20. Conciauro, G., M. Bressan, and C. Zuffada, "Waveguide modes via an integral equation leading to a linear matrix eigenvalue problem," *IEEE Trans. Microwave Theory Tech.*, Vol. 32, No. 11, 1495–1504, Nov. 1984.
  21. Cogollos, S., S. Marini, V. E. Boria, P. Soto, A. Vidal, H. Esteban, J. V. Morro, and B. Gimeno, "Efficient modal analysis of arbitrarily shaped waveguides composed of linear, circular and elliptical arcs using the BI-RME method," *IEEE Trans. Microwave Theory Tech.*, Vol. 51, No. 12, 2378–2390, Dec. 2003.
  22. Silvestre, E., M. A. Abián, B. Gimeno, A. Ferrando, M. V. Andrés, V. Boria, "Analysis of inhomogeneously filled waveguides using a biorthonormal-basis method," *IEEE Trans. Microwave Theory Tech.*, Vol. 48, No. 4, 589–596, Apr. 2000.
  23. Monsoriu, J. A., A. Coves, B. Gimeno, M. V. Andrés, E. Silvestre, "A robust and efficient method for obtaining the complex modes in inhomogeneously filled waveguides," *Microw. Opt. Tech. Letters*, Vol. 37, 218–222, May 2003.
  24. Hiptmair, R., "Higher order Whitney forms," *Progress In Electromagnetics Research*, Vol. 32, 271–299, 2001.
  25. Ding, D.-Z., R.-S. Chen, and Z. H. Fan, "An efficient SAI preconditioning technique for higher order hierarchical MLFMM implementation," *Progress In Electromagnetics Research*, Vol. 88, 255–273, 2008.
  26. Faghihi, F. and H. Heydari, "Time domain physical optics for the higher-order FDTD modeling in electromagnetic scattering from 3-D complex and combined multiple materials objects," *Progress In Electromagnetics Research*, Vol. 95, 87–102, 2009.
  27. Lai, B., N. Wang, H.-B. Yuan, and C.-H. Liang, "Hybrid method of higher-order MoM and Nyström discretization PO for 3D PEC problems," *Progress In Electromagnetics Research*, Vol. 109, 381–398, 2010.
  28. De Boor, C., *A Practical Guide to Splines*, Springer-Verlag, New York, 1978.